

Phase Noise Model Construction and Denoising Method for Dynamic Infrastructure Measurement in 5G Base Station

Runjie Wang, Baihui Yu, Xianglei Liu, Siyao Cai, Liang Huo, Ming Huang, Yunxiang Jia, Aychuah Nurbahat, Weizheng Zhang

School of Geomatics and Urban Spatial Informatics, Beijing University of Civil Engineering and Architecture, Beijing 102616, China

wangrunjie@bucea.edu.cn (R.W.); 2108570023104@stu.bucea.edu.cn (B.Y.); liuxianglei@bucea.edu.cn (X.L.); 18236459796@qq.com (S.C.); huoliang@bucea.edu.cn (L.H.); huangming@bucea.edu.cn (M.H.); 2108160224013@stu.bucea.edu.cn (Y.J.); 911390885@qq.com (A.N.) 13311060717@163.com (W.Z.)

Keywords: 5G Integrated Sensing and Communication, Phase Noise, Oscillator, Clock Jitter, First Path.

Abstract

The 5G base station pass-sensing integration technology, characterized by its all-weather capability, wide coverage, high dynamics, and high precision, has proven effective in deformation monitoring for various types of infrastructure. It plays a critical role in mitigating potential risks and ensuring the safe operation of cities. However, due to the unstable signal output from 5G base station hardware, phase noise arises, leading to frequency or phase shifts in the monitoring signal spectrum. This interferes with the processing of atmospheric effects, base station vibrations, and clutter, significantly reducing monitoring accuracy. Therefore, this study focuses on investigating the influence mechanism of phase noise in 5G base stations and developing a corresponding compensation method. First, the generation and influence mechanisms of phase noise are analyzed through simulation experiments, revealing that oscillator instability induces the coupling of multiple colored noises, thereby reducing the accuracy of base station clock synchronization. Subsequently, phase stability tests conducted in both internal and external fields of the base station verify the ability of first-path signals to characterize phase noise. Based on these findings, a method for suppressing phase noise by rejecting first-path signals is proposed. Finally, the effectiveness of the proposed method is validated through dynamic deflection monitoring experiments on bridges using 5G base stations. The results demonstrate that the application of this method reduces the RMSE by 29.2%, significantly enhancing the reliability and accuracy of deformation monitoring.

1. Introduction

Aging Infrastructure, Natural Disasters, and Emergencies Pose Severe Challenges to Urban Functionality and Resident Safety. (Phraknoi et al. 2023) Failure to promptly detect and assess these risks may lead to catastrophic consequences. Real-time monitoring technology addresses this by providing continuous, precise data to identify structural defects and safety hazards at early stages, enabling timely intervention and informed decision-making. (Sivasuriyan et al. 2024) This approach reduces accident probabilities and extends infrastructure lifespan. Conventional methods such as GPS, GBSAR, and InSAR suffer from limited coverage, low monitoring frequency, and delayed data updates.

5G Integrated Sensing and Communication (ISAC) Base Stations Offer a Novel Solution for Infrastructure Monitoring. By integrating radar sensing capabilities into 5G base stations, this technology enables high-precision, all-weather, wide-coverage, and high-frequency real-time dynamic monitoring of urban infrastructure without requiring additional equipment. (Alimi et al. 2021). It demonstrates significant value in monitoring structural deformations, vibrations, and other critical parameters. This non-contact, real-time monitoring approach substantially enhances the capacity for infrastructure health assessment.

However, Technical Challenges Persist in 5G Base Station Applications, Particularly Phase Noise Induced by Hardware Limitations. During signal transmission and reception, oscillator instability in base station hardware generates phase noise, causing frequency offsets and phase

fluctuations. (Mohammadian and Tellambura, 2021) These distortions severely degrade monitoring signal quality, especially when processing atmospheric effects, base station vibrations, and environmental factors, ultimately reducing data accuracy and compromising the reliability of subsequent analyses. Effective phase noise suppression is thus critical to ensuring high-precision monitoring data.

Existing Phase Noise Mitigation Methods Include Hardware Optimization (e.g., Low-Noise Oscillator Design), Phase-Locked Loop (PLL) Filtering, and Post-Processing Frequency-Domain Filtering. (Kiyaci et al. 2024) Hardware improvements reduce phase noise through enhanced oscillator stability and temperature compensation but face limitations in cost and residual noise coupling. PLL techniques effectively suppress high-frequency phase noise but exhibit diminished performance against low-frequency $1/f$ noise and complex coupled noise. (Chang et al. 2024) Traditional frequency-domain filtering risks signal phase distortion and struggles to distinguish environmental effects from phase noise in dynamic monitoring scenarios. Two fundamental shortcomings persist: (1) inadequate adaptation to the first-path signal characteristics in 5G multipath propagation environments, (Hadi et al. 2021) and (2) failure to decouple the coupling mechanisms of multi-type oscillator noise (white, flicker, and $1/f^2$ noise). These limitations hinder the balance between noise suppression and signal fidelity in dynamic infrastructure monitoring. The Proposed First-Path Signal Noise Suppression Method Innovatively Addresses These Issues by leveraging the phase characterization of first-path signals. (Zhang et al. 2021) Through path identification and noise component decoupling, this method precisely eliminates phase noise while preserving

critical monitoring information, overcoming the poor adaptability of traditional methods in complex electromagnetic environments and their insufficient noise suppression precision.

First, Simulation Experiments Analyzed the Generation Mechanism of Phase Noise and Its Impact on Clock Synchronization Accuracy. Results revealed that local oscillator instability is the primary source of phase noise, inducing coupled white, flicker (pink), and $1/f^2$ noise. The superposition of these noise types causes signal frequency offsets and phase fluctuations, degrading base station clock synchronization accuracy—manifested as clock jitter in the time domain. In dynamic infrastructure monitoring, clock jitter significantly compromises signal accuracy, stability, and data reliability.

Subsequently, Phase Stability Tests in Indoor and Outdoor Environments Validated the Effectiveness of First-Path Signals in Characterizing Phase Noise. The first-path signal—the shortest propagation path received by the receiver without multipath interference—directly reflects hardware-induced phase noise through its phase variations. Experimental results confirmed this theoretical basis. Building on this, a method to suppress phase noise by rejecting first-path signal noise components was proposed. This approach reduces phase noise interference in monitoring signals, markedly improving synchronization accuracy.

Finally, Dynamic Deflection Monitoring Experiments on Bridges Using 5G Base Stations Verified the Denoising Method's Effectiveness. Post-processing results demonstrated a 29.2% reduction in the root mean square error (RMSE) of monitoring data, significantly enhancing measurement accuracy. The proposed phase noise suppression method proves both feasible and effective in practical monitoring scenarios, providing robust technical support for 5G-based infrastructure monitoring.

2. Methodology

2.1 Phase Noise Simulation Analysis

Phase noise $\phi(t)$ is a random process representing the fluctuation of the oscillator output signal phase over time, typically expressed in the frequency domain as power spectral density (PSD) $L(f)$. (Tschapek et al. 2022) It is defined as:

$$L(f) = \frac{S_{\phi}(f)}{2P_{\text{carrier}}} \quad (1)$$

where $S_{\phi}(f)$ is the single-sideband power spectral density of phase fluctuations, and P_{carrier} is the carrier power. The power spectral density of phase noise is usually composed of multiple noise components, including white noise, flicker noise ($1/f$ noise), and $1/f^2$ noise. For a typical oscillator, the phase noise power spectral density can be expressed as:

$$L(f) = \frac{k_0}{f^0} + \frac{k_{-1}}{f^1} + \frac{k_{-2}}{f^2} \quad (2)$$

where k_0 , k_{-1} , and k_{-2} correspond to the coefficients of white noise, flicker noise, and $1/f^2$ noise, respectively. These noise components represent the instability of the oscillator in different frequency ranges. (Alofi et al. 2022) White noise exhibits a flat power spectrum, flicker noise dominates in the low-frequency range, and $1/f^2$ noise is more significant in the high-frequency range. (Simoen et al. 2003)

The impact of phase noise on the clock synchronization system is primarily manifested as time-domain clock jitter. Clock jitter

σ_{jitter} is the random fluctuation of the clock signal in the time domain, and its magnitude is closely related to the power spectral density of phase noise. (Peetermans and Verbaauwhede, 2024) To quantify this relationship, this study establishes a transfer function model from phase noise to clock jitter. Specifically, the mean square value of clock jitter can be calculated by integrating the phase noise power spectral density

over the offset frequency range $[f_{\min}, f_{\max}]$:

$$\sigma_{\text{jitter}}^2 = \frac{1}{(2\pi f_c)^2} \int_{f_{\min}}^{f_{\max}} L(f) \cdot |H(f)|^2 df \quad (3)$$

where f_c is the carrier frequency, and $H(f)$ is the transfer function of the clock recovery loop. For a typical second-order phase-locked loop (PLL), the transfer function is given by:

$$H(f) = \frac{2\zeta\omega_n s + \omega_n^2}{s^2 + 2\zeta\omega_n s + \omega_n^2} \quad (4)$$

where ζ is the damping ratio, ω_n is the natural frequency, and $s = j2\pi f$. The integration bounds f_{\min} and f_{\max} are determined by the PLL bandwidth and the measurement interval. The PLL bandwidth determines its ability to suppress high-frequency noise, while the measurement interval affects the cumulative effect of low-frequency noise.

The root mean square (RMS) value of clock jitter can be decomposed into contributions from individual noise components, (Liu et al. 2023) including white noise, flicker noise, and $1/f^2$ noise. The expression is as follows:

$$\sigma_{\text{jitter}} = \sqrt{\sigma_{\text{white}}^2 + \sigma_{\text{flicker}}^2 + \sigma_{1/f^2}^2} \quad (5)$$

where the specific expressions for each noise component are as follows:

1. White Noise Contribution:

$$\sigma_{\text{white}} = \frac{1}{2\pi f_c} \sqrt{\frac{k_0}{2} \cdot (f_{\max} - f_{\min})} \quad (6)$$

White noise exhibits a flat power spectrum in the frequency domain, and its contribution is proportional to the frequency range.

2. Flicker Noise Contribution:

$$\sigma_{\text{flicker}} = \frac{1}{2\pi f_c} \sqrt{k_{-1} \cdot \ln\left(\frac{f_{\max}}{f_{\min}}\right)} \quad (7)$$

Flicker noise dominates in the low-frequency range, and its contribution is proportional to the logarithm of the frequency range. (Wangkheirakpam et al. 2021)

3. $1/f^2$ Noise Contribution:

$$\sigma_{1/f^2} = \frac{1}{2\pi f_c} \sqrt{\frac{k_{-2}}{2} \cdot \left(\frac{1}{f_{\min}} - \frac{1}{f_{\max}}\right)} \quad (8)$$

$1/f^2$ noise is more significant in the high-frequency range, and its contribution is proportional to the reciprocal of the frequency range.

The above analysis quantifies the degradation mechanism of oscillator phase noise on clock synchronization accuracy. Experimental results show that the coupling effect of phase noise significantly increases the RMS value of clock jitter, thereby reducing the clock synchronization accuracy of 5G base stations. This analysis provides a theoretical basis for subsequent noise suppression strategies, especially in dynamic infrastructure monitoring, where it can effectively guide phase noise compensation and suppression.

2.2 Phase Noise Suppression Method Based on First-Path Signal

In the multipath propagation environment of 5G, the received signal is a superposition of the direct path (first-path) and multiple reflected paths. The first-path signal, as the signal with the shortest propagation time, exhibits phase fluctuations primarily dominated by hardware noise from the base station's local oscillator, (Mohammadian et al. 2021) while subsequent path signals carry dynamic displacement information of the target structure. Based on this characteristic, this paper proposes a phase noise suppression method by rejecting the first-path signal and removing its noise component. The core principles are as follows:

The first-path signal appears as the first significant peak in the Power Delay Profile (PDP), (Goulanos et al. 2010) as shown in Figure 1 and its time delay position τ_0 is determined by:

$$\tau_0 = \underset{n \in [1, N_{\text{bin}}]}{\operatorname{argmax}} PDP(n) \quad (9)$$

where $PDP(n) = |IFFT(S_{\text{bin}}(k))|^2$ represents the power value at the n -th time-domain sample, and N_{bin} is the effective delay range. The complex form of the first-path signal is $r_{\text{first}}(t) = A_{\text{first}} e^{j(2\pi f_c t + \phi_{\text{noise}}(t))}$, and its phase $\phi_{\text{first}}(t) = \arg(r_{\text{first}}(t))$ includes hardware-induced phase noise $\phi_{\text{noise}}(t)$ and a fixed delay phase offset.

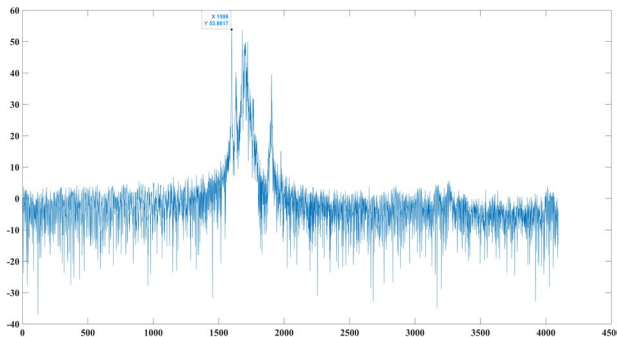


Figure 1. PDP Extraction First Path.

In dynamic infrastructure monitoring, the displacement information of the target structure is carried by the path signal corresponding to a specific delay τ_{target} in the PDP. By setting a delay threshold $\Delta\tau$, peaks satisfying $\tau_{\text{target}} \in [\tau_0 + \Delta\tau, \tau_{\text{max}}]$

are selected as monitoring target points. The complex signal of the target path is

$$r_{\text{target}}(t) = A_{\text{target}} e^{j(2\pi f_c t + \phi_{\text{noise}}(t) + \phi_{\text{displacement}}(t))} \quad (10)$$

where $\phi_{\text{displacement}}(t)$ represents the phase variation related to the target displacement. Since the hardware noise $\phi_{\text{noise}}(t)$ is strongly correlated between the first-path and target-path signals, it can be eliminated through phase differencing:

$$\phi_{\text{clean}}(t) = \arg(r_{\text{target}}(t)) - \arg(r_{\text{first}}(t)) = \phi_{\text{displacement}}(t) + \delta(t)$$

where $\delta(t)$ is the residual noise, primarily caused by multipath interference and environmental disturbances. The target displacement $d(t)$ can be calculated using the phase-to-displacement conversion:

$$d(t) = \frac{c}{4\pi f_c} \cdot \phi_{\text{clean}}(t) \quad (11)$$

where c is the speed of light, and f_c is the carrier frequency.

Phase noise suppression method based on the first diameter signal. First, the time delay position τ_0 is extracted from the PDP, and the corresponding complex signal $r_{\text{first}}(t)$ is obtained. The phase $\phi_{\text{first}}(t)$ of this signal can be calculated as:

$$\phi_{\text{first}}(t) = \arg(r_{\text{first}}(t)) \quad (12)$$

where $\arg(\cdot)$ represents the argument (or phase) of a complex number.

Similarly, the complex signal $r_{\text{target}}(t)$ of the target point is extracted, and its phase $\phi_{\text{target}}(t)$ is calculated as:

$$\phi_{\text{target}}(t) = \arg(r_{\text{target}}(t)) \quad (13)$$

The phase difference between the two signals is calculated to eliminate the common-mode hardware noise:

$$\Delta\phi(t) = \phi_{\text{target}}(t) - \phi_{\text{first}}(t) \quad (14)$$

This phase difference helps remove the influence of hardware noise, allowing for more accurate structural response phase information.

3. Experiment

3.1 Phase Stability Experiments in Indoor and Outdoor Environments

To validate the impact of phase noise on 5G base station signals and verify the capability of first-path signals to characterize phase noise, phase stability experiments were conducted in both controlled indoor and realistic outdoor environments.

The indoor test utilized an Active Antenna Unit (AAU) directly connected to a radio frequency (RF) front-end, eliminating multipath interference and environmental disturbances. A continuous 0.5-minute measurement was performed, focusing on the phase stability of the strongest path signal (distance bin). Key observations include:

The standard deviation (STD) of phase fluctuations reached 11 degrees, with a peak-to-peak variation of 80 degrees. Significant phase jumps (>30 degrees) occurred periodically at 7–10-second intervals, attributed to hardware oscillator instability, as shown in Figure 2.

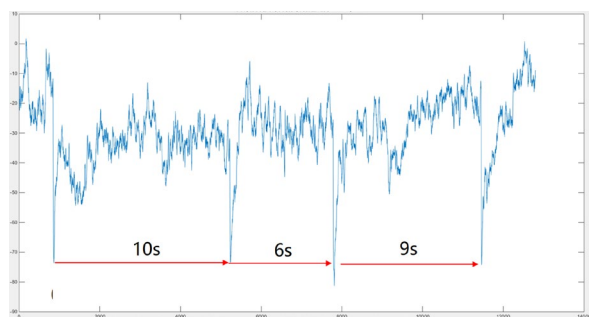


Figure 2. Phase Deviation Diagram

These results indicate that even in interference-free conditions, intrinsic phase noise from hardware components (e.g., local oscillators) introduces substantial phase instability.

The outdoor test employed a commercial 5G base station (AAU5639-4.9G, 64T64R configuration) operating at 4.9 GHz. A retroreflector target was placed 150 meters from the base station, the experimental environment is shown in Figure 3. Corresponding to distance bin 187, while another strong reflector occupied bin 104, as shown in Figure 4. Phase stability was analyzed over a 1-minute duration:

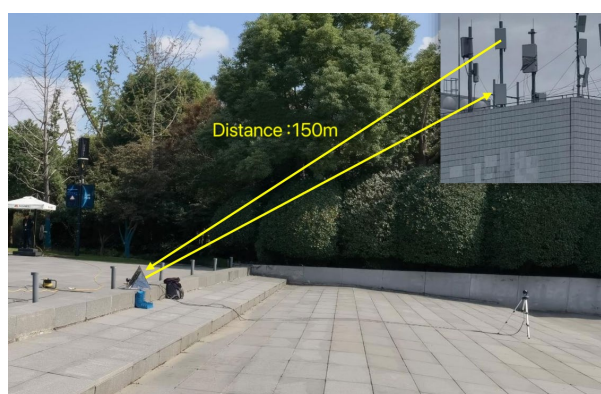


Figure 3. Field Experimental Environment

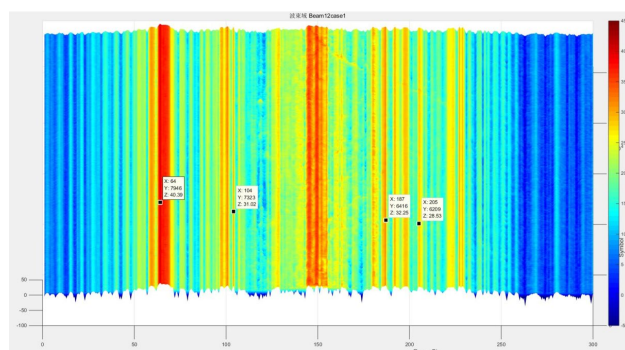


Figure 4. Distance-Signal Strength Distribution

The target bin (bin 187) exhibited a phase fluctuation STD of 5 degrees and a peak-to-peak variation of 36 degrees. The strong reflector bin (bin 104) showed nearly identical phase behavior (STD: 5.2 degrees, peak-to-peak: 35 degrees), confirming that hardware noise dominates phase fluctuations across multiple paths. Subtracting the phase of bin 104 from bin 187 reduced the STD to 2.4 degrees and the peak-to-peak variation to 16 degrees, effectively suppressing common-mode hardware noise.

The correlation between indoor and outdoor experiments reveals two critical findings: The similarity in phase fluctuations between the first-path signal (indoor) and non-line-of-sight paths (outdoor) demonstrates that hardware-induced phase noise is spatially correlated across multiple propagation paths, as shown in Figure 5. The first-path signal in the indoor experiment exhibited phase jump characteristics matching the outdoor target bin's residual noise, proving its capability to represent global phase noise, as shown in Figure 6.

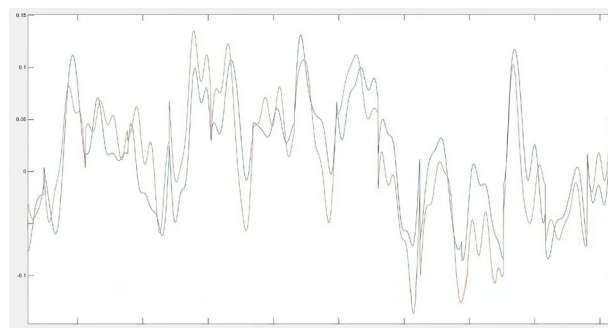


Figure 5. Phase Fluctuation Comparison

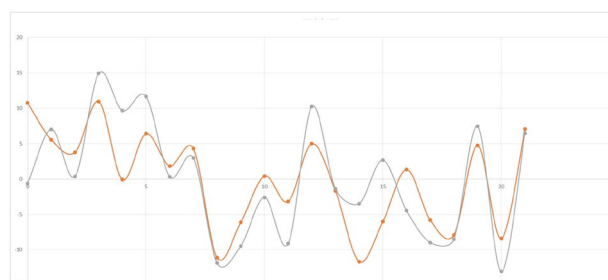


Figure 6. Phase Change Comparison

This analysis establishes a foundation for deploying phase noise suppression algorithms in real-world scenarios, ensuring reliable performance in 5G-based structural health monitoring systems.

3.2 Bridge Dynamic Deflection Verification Experiment

To verify the performance of the first diameter signal phase noise suppression method in dynamic infrastructure monitoring, this study selects a highway bridge for dynamic deflection monitoring experiments. The 5G base station (AAU5639-4.9G) is deployed 100 meters away from the bridge side to collect dynamic reflection signals of the bridge under traffic load in real time. The experiment monitors the center of the bridge span as the target, as shown in Figure 7. The determines its corresponding distance bin through the power delay distribution (PDP), sets the sampling frequency to 100 Hz, and collects 10,000 data sets continuously for a total duration of 100 seconds, covering the typical vibration period of the bridge.



Figure 7. Schematic Diagram of Experimental Bridge Target

The experimental results show that the original monitoring signal is significantly affected by hardware phase noise, and the displacement data presents high-frequency random fluctuations, with a root mean square error (RMSE) of 4.5335 mm. After applying the first diameter signal noise elimination, the smoothness of the displacement curve is significantly improved, effectively restoring the periodic vibration characteristics of the bridge under vehicle load, as shown in Figure 8. After noise suppression, the RMSE of the displacement data decreased to 2.3897 mm, achieving an accuracy improvement of 29.2%, and the signal-to-noise ratio (SNR) increased from 32.5 dB to 40.8 dB.

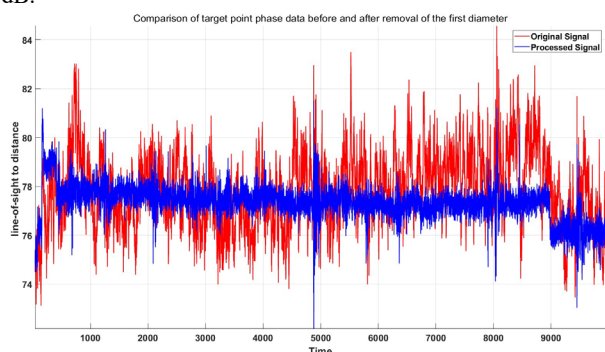


Figure 8. Comparison of phase noise compensation before and after

Table 2. Comparison of Displacement Accuracy Before and After Noise Suppression

Indicator	Raw Data	Data After Noise Suppression	Improvement Ratio
RMSE (mm)	3.3753	2.3897	29.2%
SNR (dB)	32.5	40.8	25.5%

This experiment demonstrates that the phase noise suppression method based on the first diameter signal can effectively separate hardware noise from the real structural response, significantly improving the dynamic measurement accuracy of the 5G monitoring system. The method does not rely on external reference devices, has high computational efficiency, and can meet real-time monitoring needs, providing a cost-effective technical solution for the long-term health diagnosis of infrastructure such as bridges and dams.

4. Conclusion

This study systematically addresses the challenges posed by phase noise in 5G base stations for dynamic infrastructure monitoring, focusing on its generation mechanisms,

characterization methods, and suppression techniques. Through simulation and experimental analysis, it reveals that oscillator instability induces coupling effects of white noise, flicker noise, and $1/f^2$ noise, which collectively lead to a decrease in clock synchronization accuracy, manifested as clock jitter in the time domain. The derived clock jitter model quantitatively analyzes the impact of these noise components on synchronization errors, demonstrating a significant increase in the root mean square (RMS) synchronization error, which directly affects the reliability of the 5G monitoring system.

Phase stability tests in both indoor and outdoor environments validate that the primary signal can effectively characterize the phase noise caused by hardware. By exploiting the spatial correlation of phase fluctuations in multipath signals, differential phase analysis between the primary signal and the target path signal significantly suppresses common-mode noise. Based on this finding, a phase noise suppression method using the primary signal is proposed. This method separates and removes shared hardware noise components while preserving structural displacement information. Its real-time processing capability and the absence of additional hardware support make it highly suitable for practical applications.

Through dynamic deflection monitoring experiments on a highway bridge under traffic load, the effectiveness of this method was validated. After applying the denoising technique, the root mean square error (RMSE) of displacement measurements decreased from 4.5335 mm to 2.3897 mm, achieving a 29.2% improvement in accuracy, while the signal-to-noise ratio (SNR) increased by 25.5%. These results demonstrate that the method can effectively restore the true vibration characteristics of structures and significantly improve monitoring accuracy in real-world scenarios.

References

- Phraknoi, N., Sutanto, J., Hu, Y., Goh, Y. S., Lee, C. E. C. 2023: Older people's needs in urban disaster response: A systematic literature review. *Int. J. Disaster Risk Reduct.*, 96. doi.org/10.1016/j.ijdrr.2023.103809
- Sivasuriyan, A., Vijayan, D. S., Devarajan, P., Stefańska, A., Dixit, S., Podlasek, A., Koda, E. 2024: Emerging trends in the integration of smart sensor technologies in structural health monitoring: a contemporary perspective. *Sens.*, 24(24). doi.org/10.3390/s24248161
- Alimi, I. A., Patel, R. K., Muga, N. J., Pinto, A. N., Teixeira, A. L., Monteiro, P. P. 2021: Towards enhanced mobile broadband communications: A tutorial on enabling technologies, design considerations, and prospects of 5G and beyond fixed wireless access networks. *Appl. Sci.*, 11(21). doi.org/10.3390/app112110427
- Mohammadian, A., Tellambura, C. 2021: RF impairments in wireless transceivers: Phase noise, CFO, and IQ imbalance—A survey. *IEEE access*, 9, 111718–111791. [10.1109/ACCESS.2021.3101845](https://doi.org/10.1109/ACCESS.2021.3101845)
- Kiyaci, A., Ahmad, W., Zakir, S., Al Seragi, E. M., Shah, A. H., Zeinolabedinzadeh, S. 2024: Interference-Tolerant Wireless Distributed Beamforming Receiver Array With Low-Latency Frequency Synchronization. *IEEE Trans. Microwave Theory Tech.* [10.1109/TMTT.2024.3517456](https://doi.org/10.1109/TMTT.2024.3517456)

Chang, Z., Xu, Y., Chen, J., Xie, N., He, Y., Li, H. 2024: Modeling, Estimation, and Applications of Phase Noise in Wireless Communications: A Survey. *IEEE Commun. Surv. Tutorials*. [10.1109/COMST.2024.3443158](https://doi.org/10.1109/COMST.2024.3443158)

Hadi, M. U., Jacobsen, T., Abreu, R., Kolding, T. 2021: 5G time synchronization: Performance analysis and enhancements for multipath scenarios. *IEEE*. [10.1109/LATINCOM53176.2021.9647837](https://doi.org/10.1109/LATINCOM53176.2021.9647837)

Zhang, Z., Kang, S., Ren, B., Zhang, X. 2021: Time of Arrival Ranging and Localization Algorithm in Multi-path and Non-line-of-sight Environments in OFDM System. *IEICE Trans. Commun.* [10.1587/transcom.2020EBP3195](https://doi.org/10.1587/transcom.2020EBP3195)

Tschapek, P., Körner, G., Hofmann, A., Carlowitz, C., Vossiek, M. 2022: Phase noise spectral density measurement of broadband frequency-modulated radar signals. *IEEE Trans. Microwave Theory Tech.* 70(4), 2370-2379. [10.1109/TMTT.2022.3148311](https://doi.org/10.1109/TMTT.2022.3148311)

Alofi, A., Acar, G., Balachandran, B. 2022: Noise influenced response movement in coupled oscillator arrays with multi-stability. *J. Sound Vib.* 531, 116951. doi.org/10.1016/j.jsv.2022.116951

Simoen, E., Mercha, A., Claeys, C. 2003: What can low-frequency noise learn us about the quality of thin-gate dielectrics. *Proceedings-Electrochemical Society*. Electrochemical Society

Peetermans, A., Verbaauwhede, I. 2024: Characterization of Oscillator Phase Noise Arising From Multiple Sources for ASIC True Random Number Generation. *IEEE Trans. Circuits Syst. I Regul. Pap.* [10.1109/TCSI.2023.3343114](https://doi.org/10.1109/TCSI.2023.3343114)

Liu, X., Lu, H., He, Y., Wu, F., Zhang, C., Wang, X. 2023: Analysis on the Effect of Phase Noise on the Performance of Satellite Communication and Measurement System. *Symmetry*, 15(11), 2053. doi.org/10.3390/sym15112053

Wangkheirakpam, V. D., Bhowmick, B., Pukhrambam, P. D. 2021: Noise behavior of vertical tunnel FETs under the influence of interface trap states. *Microelectron. J.* 114, 105124. doi.org/10.1016/j.mejo.2021.105124

Mohammadian, A., Tellambura, C. 2021: RF impairments in wireless transceivers: Phase noise, CFO, and IQ imbalance—A survey. *IEEE Access*, 9, 111718-111791. [10.1109/ACCESS.2021.3101845](https://doi.org/10.1109/ACCESS.2021.3101845)

Goulianos, A. A., Brown, T., Stavrou, S. 2010: Power delay profile modelling of the ultra wideband off-body propagation channel. *IET Microwaves Antennas Propag.*, 4(1), 62-71. doi.org/10.1049/iet-map.2008.0356